J. Chem. Soc., Faraday Trans. 1, 1988, **84**(4), 1223–1242

Combined Study of Coagulation Kinetics and Close-range Aggregate Structure

Alexander Lips*
Unilever Research, Colworth Laboratory, Sharnbrook, Bedford MK 44 1LQ

Ralph M. Duckworth
Unilever Research, Port Sunlight Laboratory, Wirral, Merseyside L62 4XN

The kinetics of coagulation of model polystyrene latex spheres under both reaction and diffusion control have been studied. The zeroth moment of the aggregate distribution has been measured by an automated laser particle-counting method, and the second moment by time-resolved low-angle light scattering. Emphasis has been both on dimer formation and the longer-time kinetics of cluster–cluster aggregation. Extension of the light scattering method of Giles and Lips (*J. Chem. Soc., Faraday Trans. 1*, 1974, **74**, 733) has yielded information on the close-range structure in growing aggregates. The moments of the aggregate distribution can deviate from the predictions of the simple Smoluchowski constant-kernel equation. Acceleration in rate from reaction to diffusion control can occur in so-called rapid coagulation and in an intermediate regime of slow coagulation. In very slow coagulation, the rate decelerates, suggesting transition from reaction to equilibrium control. Interpretation on kinetic random polycondensation theory for an RA_f process has yielded effective functionalities f which increase with particle density and decrease with increasing reaction control. The potential of spherical particles for high functional reactivity is not in general realised because aggregates can rearrange within the timescale of collisions, and spheres can form cycles (ring-closed structures) as early as the trimer stage, with consequent wastage of functionalities. The close-range structure of aggregates increases in compactness with increasing reaction control and decreasing particle concentration. The kinetics in the regime of the very slow coagulation are consistent with an initial reversible step of dimerisation followed by the irreversible formation of higher-order aggregates with ring-closed bonding. Application of reversible polycondensation theory to the dimer step has enabled the strength of attraction, a finite primary minimum, to be quantified. The observed deviations from constant-kernel Smoluchowski kinetics have important implications for the measurement of classical colloid stability plots and may be the origin of the discrepancies between the predictions of DLVO theory and kinetic measurements of colloid stability.

To colloid scientists, the most familar theoretical idea in the field of aggregation kinetics is the Smoluchowski equation,[1]

$$\frac{\mathrm{d}c_m}{\mathrm{d}\tau} = \frac{1}{2}\sum_{i+j=m}^{\infty} K_{ij}\,c_i\,c_j - c_m \sum_{j=1}^{\infty} K_{mj}\,c_j \tag{1}$$

which represents the unidirectional, irreversible aggregation of colloid particles. Here $c_m(\tau)$ is the number concentration of m-fold aggregates at reduced time τ, scaled for convenience to an initial condition $c_m(0) = \delta_{m1}$ which implies unit initial monomer concentration and $\sum mc_m(\tau) = 1$. The coagulation kernel K_{ij} represents the bimolecular rate constant for the association between i and j. Smoluchowski considered that a constant kernel, independent of i and j, could reasonably represent the case of diffusion-limited Brownian aggregation. Then simple expressions hold for the zeroth, first and second moments of the aggregate distribution

$$\left.\begin{aligned} M_0 &= \sum c_m = 1/(1+2\tau) \\ M_1 &= \sum m c_m = 1 \\ M_2 &= \sum m^2 c_m = 1+4\tau. \end{aligned}\right\} \quad [c_m(0) = \delta_{m1}] \qquad (2)$$

In general $\tau = A^+ c_0\, t$, where c_0 is the initial monomer concentration (assumed to be monodisperse), t is the time of coagulation and A^+ is a system-specific forward rate constant. For strictly diffusion-limited aggregation, A^+ is half the so-called rapid rate constant ($= 4\boldsymbol{k}T/3\eta$, where $\boldsymbol{k}$ is the Boltzmann constant, T is the temperature and η is the viscosity of the solvent).

The Smoluchowski equation, with the approximation of constant coagulation kernel, has served as a theoretical framework for an extensive literature on the stability of dilute colloids. Studies in this area have concentrated on both rapid coagulation in the diffusion limit,[2-5] including the retardation due to hydrodynamic forces at short range,[6,7] and slow coagulation in the presence of interparticle repulsive forces. In the latter case it has been usual to employ the Fuchs modification[8] of the original Smoluchowski diffusion treatment to relate the reduction in aggregation rate relative to the diffusion limit to the nature of the repulsive pair potential. Kinetic stability studies have provided the first means of testing some of the predictions of DLVO theory. This has been by way of the classical log W *vs.* log C plots,[9-13] where the stability factor W represents the inverse ratio of the rate observed at electrolyte concentration C to that in the rapid diffusion limit in excess C.

There are substantial quantitative discrepancies between the predictions of DLVO theory and colloid stability measurements. Experimental log W *vs.* log C plots show an unexpected dependence on particle radius,[9-11] and inferred Hamaker constants can be unrealistic in magnitude and in their apparent strong variation with ionic strength.[9,11,13] These discrepancies are not successfully explained in terms of refinement of either electrostatic theory or dispersion forces, or by inclusion of hydrodynamic forces.[6,7] Duckworth and Lips[14] have developed the Reerink and Overbeek[9] use of the Fuchs theory by incorporating more recent dispersion theory, with low-frequency contributions and screening by electrolyte, and by including the concept of a Stern layer. The latter can account satisfactorily for the apparent variation in inferred Hamaker function with electrolyte, but cannot explain the observed dependence on particle radius.

From an experimental viewpoint, the measurement of colloidal aggregation is generally difficult. Early studies utilised ultramicroscopy,[15-17] and despite the tedium and inherent difficulties of this approach it was possible to provide support for the predictions of the Smoluchowski theory. Subsequent automation of a direct counting approach for sub-microscopic particles, using a flow cell with hydrodynamic focussing and individual detection of light scattered from each of the kinetic units, was first achieved by Derjaguin and Kudryavetseva.[18] Subsequent refinement of this approach now permits measurements not only of the total number of kinetics units but also the details of the aggregate distribution.[5,19-22] It is the more recent studies[20,22] which have convincingly highlighted deviations from strict Smoluchowski behaviour and as such support earlier inferences.[5,18,24]

Bulk light scattering techniques, by virtue of their greater experimental simplicity, have been more commonly employed than direct counting methods. These include turbidity,[2] scattered light intensity[3,23,24] and autocorrelation of the scattered light.[25] Interpretation of such measurements has usually implied the validity of Smoluchowski kinetics, although this is not an essential constraint. At sufficiently low angles, light scattering reflects the second moment, M_2, of the aggregate size distribution, and Lips and Willis,[3] using low-angle scattering, were able to demonstrate a linear time dependence for M_2 consistent with the Smoluchowski assumption [eqn (2)]. A more general representation of light scattering moments has been developed by Giles and Lips,[24] enabling coagulation rate constants to be inferred from the simpler measurement at wide angles.

Recently, analytical solutions of the Smoluchowski equation [eqn (1)] have been developed for non-constant kernels of the type $K_{ij} = i+j$ and $K_{ij} = (ij)^w$, where $0 < w < 1$.[26,27] Some of these had their origin in kinetic theories of polymerisation first considered by Dostal and Raff,[28] Stockmayer,[29] and recently Dusek[30] and Ziff and Stell.[31] Kinetic approaches to the polymerisation of f-functional monomer units can provide isomorphous solutions to those of the statistical theory of Flory–Stockmayer (FS).[29] Ziff and Stell[31] have shown that the solutions of eqn (1) for kernel $K_{ij} = [(f-2)i+2][f-2)j+2]$ retain the canonical form of FS theory and represent the kinetics of a classical RA_f polymerisation. The case $f = 2$ has constant kernel ($K_{ij} = 4$) and is therefore isomorphous to the Smoluchowski diffusion limit; $f > 2$ indicates an increase in reactivity as clusters grow, leading to gel formation at critical gel time $\tau_c = 1/f(f-2)$ and divergence in the second and higher moments of the aggregate distribution.

The idea of modelling colloidal systems in terms of statistical polycondensation theory has been developed recently by Cohen and Benedek,[32] who suggested that the equilibrium distributions of colloidal aggregates are isomorphous to that of an RA_f polymer system in the limit of high functionality ($f \to \infty$). It is assumed that particles in aggregates do not form cycles (rings of 'bonded' monomers) and that reactive sites have *a priori* equal reactivity. Cohen and Benedek suggest further that colloid particles cannot realise their potential for high functional bonding when diffusion-limited kinetics apply. Then, for kinetic reasons the evolution of the aggregate distribution, in the early stages far from equilibrium, behaves as though it were close to an $f = 2$ scheme isomorphous to the Smoluchowski model. The detailed measurements of aggregate distributions by Bowen *et al.*[33] support these arguments, indicating behaviour close to $f = 2$ behaviour in the kinetic regime, and the characteristics of high f bonding as the coagulation evolves towards equilibrium. Lips[34] has further developed the analogy of Smoluchowski kinetics with an RA_f statistical process and has adapted a cascade model by Kajiwara *et al.*[35,36] to represent the light scattering moments of the aggregate distribution from coagulating colloidal spheres.

In this paper we present the results of an extensive series of measurements of the rapid and slow coagulation of a model polystyrene latex. In the main this has involved studies of the zeroth moment M_0 of the aggregate distribution by an automated particle-counting technique. Measurements of the second moment M_2, by low-angle light scattering, and of aggregate structure, by wide-angle scattering, are also presented. We find that these moments do not strictly conform to Smoluchowski kinetics, consistent with inferences from recent, direct measurements of aggregate distributions.[33] One aim of this paper is to examine these deviations in terms of the more recent theories cited above. The second aim is to point out their important consequences for the measurement and interpretation of log W *vs.* log C stability plots. We observe satisfactory agreement with DLVO theory when it is possible to measure initial kinetics, effectively in the two-particle regime, which is the condition of classical theory. When this regime cannot be accessed, as has frequently been the case, then non-conformity to simple Smoluchowski kinetics is a likely cause of observed disagreement between theory and experiment.

Experimental

The monodisperse polystyrene latex predominantly used in this study was prepared by the method of Kotera *et al.*[37] and had an EM diameter of 168 nm. The light scattering method of Lips *et al.*[23] was used to ascertain the absence of pre-aggregation in the latex prior to the coagulation experiments. A limited range of experiments (light scattering) was also performed on a 207 nm polystyrene latex, also prepared by the method of Kotera *et al.*

The light scattering coagulation studies involved the use of a conventional Sofica wide-angle instrument, with incoherent source and detection, and also the spatially coherent optics and detection system of a Malvern Autocorrelator with illumination provided by a 5 mW He/Ne Spectra Physics laser. Non-standard use of the Malvern optics was made at a low scattering angle of 3° to monitor the evolution of the second moment M_2 of the aggregate distribution. In this case a beam stop was insterted to prevent direct incidence of the main beam on the photomultiplier tube. For the more strongly scattering dispersions, at high number concentration $c_0 > 10^9\ \mathrm{cm^{-3}}$, the problems of flare, dust *etc.*, usually severe in low-angle scattering, were found not to be limiting. Although it was not possible to measure absolute rate constants, reliable estimates could be made of the degree of curvature, if any, in the time-dependence of M_2.

Particle-counting measurements of M_0 were made using an automatic particle counter. This instrument was based on one previously described,[4,5] but its sensitivity had been increased by detection of scattered light at 45° rather than 90°, and the use of a more powerful laser (2 W argon, Spectra Physics).

All measurements were made at 25 °C.

Results and Discussion

Rapid Coagulation

A typically curved $1/\sum c_m$ *vs.* t plot, obtained by particle counting, is shown in fig. 1. The complete set of particle-counting data for rapid coagulation is summarised in fig. 2, conveniently represented in terms of reduced variables, namely the zeroth moment of the distribution $M_0\ (=\sum c_m/c_0)$ and the reduced coagulation time $Kc_0\,t$. ($K = 6.1 \times 10^{-18}\ \mathrm{m^3\ s^{-1}}$ is the value of the rapid rate constant in water at 25 °C, corresponding to the theoretical diffusion limit.) The data span the range of initial number density c_0, 2×10^7 to $6\times10^8\ \mathrm{cm^{-3}}$, also studied by other workers.[4,5] Fig. 2 shows increasing curvature in M_0 with increasing initial number density. At the lowest c_0, an initial slower rate (30% of the maximum diffusion rate) persists to long times with no curvature apparent; as c_0 increases, however, this regime of slower kinetics progressively narrows and the rate accelerates to a limiting condition which appears to be linear with time and has a slope close to that expected for the maximum Smoluchowski diffusion rate.

It is instructive to compare our data with those of previous workers. Derjaguin and Kudryavetseva[18] found deviations from Smoluchowski kinetics in the rapid coagulation of gold sols. Recent direct studies of aggregate distributions[20,22,33] have shown this convincingly also for polystyrene latex. Earlier Hatton *et al.*,[4] by direct particle counting, observed a dependence of the rate constant on the number density but did not attribute this to deviations from strict Smoluchowski kinetics. Lips and Willis,[3] using low-angle light scattering, and Lichtenbelt *et al.*,[2] using stopped-flow turbidimetry, inferred rate constants that were independent of number density. On the basis of our work it is possible to offer a unifying explanation for these observations, *viz.* any apparent contradictions are the consequence of disregard for more complex kinetics than the simplest approximation of constant kernel K_{ij}. If this is (erroneously) assumed

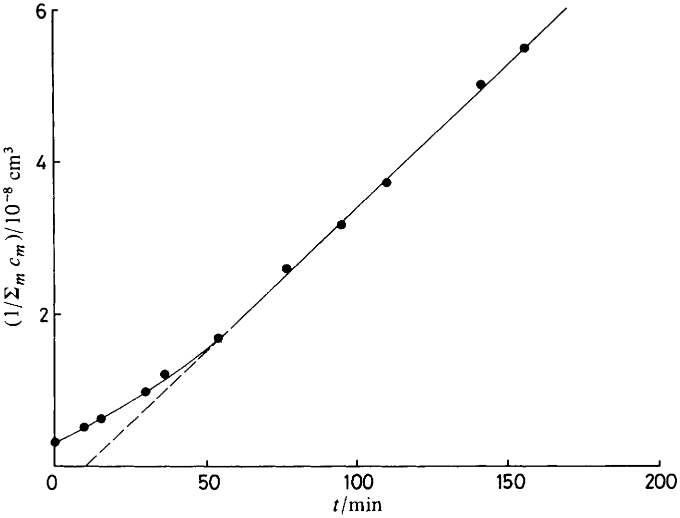

Fig. 1. Rapid coagulation. Typical dependence of inverse particle concentration $(1/\Sigma_m c_m)$ on time. (25 °C, $c_0 = 3.17 \times 10^8$ cm^{-3}, 0.3 mol dm^{-3} sodium chloride, latex 167 nm).

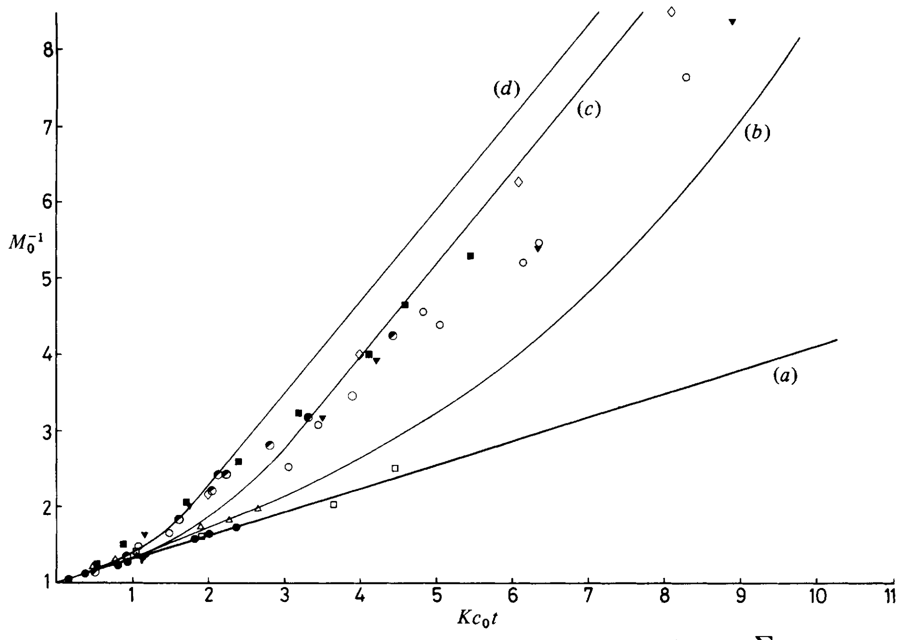

Fig. 2. Rapid coagulation: variation of inverse zeroth moment M_0^{-1} $(= c_0/\Sigma_m c_m)$ with reduced coagulation time $Kc_0 t$ for a range of particle concentrations, c_0 (cm^{-3}): ●, 2.17×10^7; □, 2.21×10^7; △, 4.35×10^7; ◐, 7.57×10^7; ■, 1.06×10^8; ○, 2.11×10^8; ▼, 3.17×10^8 and ◇, 5.50×10^8. Full curves are based on kinetic polycondensation theory [eqn (3)] fitted on the basis of common initial slope for all particle densities with functionality f: (a) $f = 2$, (b) $f = 2.5$, (c) $f = 4$, (d) $f = 10$. (25 °C, 0.3 mol dm^{-3} sodium chloride, latex 167 nm, $K = 6.12 \times 10^{-18}$ m^3 s^{-1}).

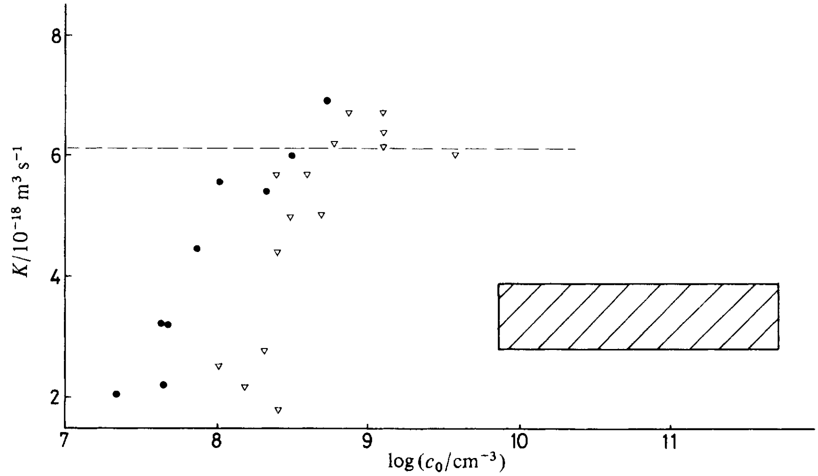

Fig. 3. Rapid rate constants inferred by different techniques: ●, particle counting; ▽, time-resolved light scattering at 30° scattering angle (both for 167 nm latex, 25 °C, 0.3 mol dm^{-3} sodium chloride). The shaded area represents the range of results obtained by Lichtenbelt *et al.*[2] using stopped-flow turbidimetry; (---) theoretical Smoluchowski value.

then at best only average rate constants can be inferred. These moreover can be technique-dependent, as is shown in fig. 3. The minimum times for measurement are typically of the order of 0.1 s, 10 s, and 10^2 s, respectively for stopped-flow turbidity, conventional time-resolved incoherent light scattering and particle counting. Since all the curves in fig. 2 tend to the same initial slope, it is reasonable that the results of the fastest-responding technique, stopped flow, show the least dependence of effective rate constant on number density. The relatively long-time dead times in particle counting, on the other hand, imply that the common initial regime can be accessed only at very low number concentrations; beyond $c_0 > 5 \times 10^7$ cm^{-3} it is not possible to observe the initial process of dimer formation. The measurement is then biased to higher-order processes which do not conform to the approximation of constant kernel. The results based on conventional light scattering lie, as expected, between these extremes. Since at very low c_0 the kinetic plots in fig. 2 show little curvature, this study still supports those earlier particle counting[4,5] and low-angle light scattering studies[3] in which c_0 was confined to $< 5 \times 10^7$ cm^{-3}, and second-order kinetics was demonstrated, with rate constants between one third and one half of the Smoluchowski diffusion value.

Slow Coagulation

Deviations from second-order kinetics can be more pronounced and varied in slow coagulation. Fig. 4 and 5 depict particle-counting data in which there is striking curvature in the $1/\sum c_m$ *vs.* t plots, qualitatively similar to that for rapid coagulation. Low-angle light scattering data, representing the second moment M_2 ($= \sum m^2 c_m/c_0$) of the aggregate distribution, are similarly curved, as shown in fig. 6. This acceleration of rate is observed for electrolyte concentrations C in the intermediate range, 0.05–0.1 mol dm^{-3}, adjacent to the critical coagulation concentration (0.14 mol dm^{-3}). On the other hand, for $C < 0.05$ mol dm^{-3} (regime of very slow coagulation) deceleration in the kinetics occurs, as illustrated in fig. 7.

These features have important ramifications for the construction of log W *vs.* log C stability plots. Fig. 8 shows a typical plot obtained by conventional light scattering. The data for two different particle densities lie on the same curve, confirming that the chosen

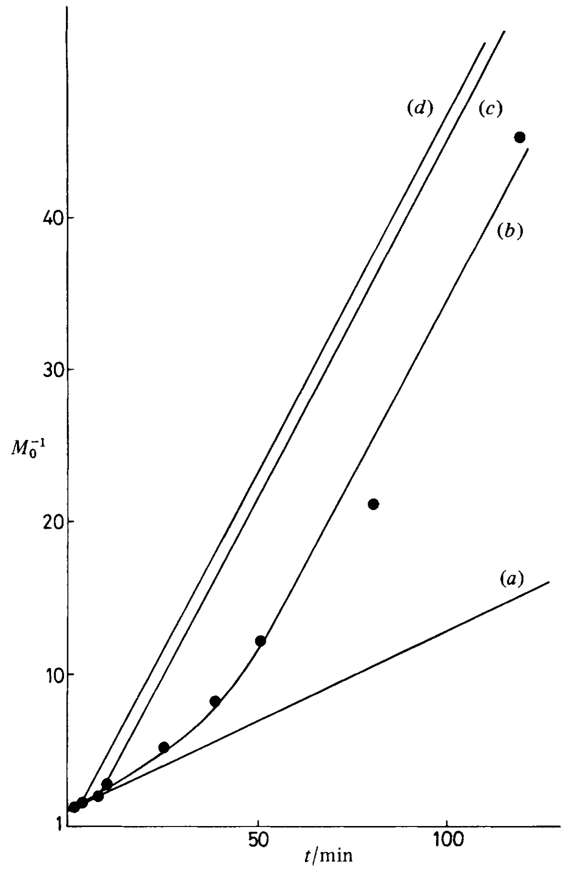

Fig. 4. Intermediate regime of slow coagulation. Variation of inverse zeroth moment $M_0^{-1}(=c_0/\sum_m c_m)$ with time. Full curves represent eqn (3) fitted on the basis of common initial slope with functionality f as marked. (25 °C, $c_0 = 3.7 \times 10^9$ cm^{-3}, 0.065 mol dm^{-3} sodium chloride, latex 167 nm). (a) $f = 2$, (b) $f = 2.16$, (c) $f = 3$, (d) $f = 10$.

method is sensitive only to initial kinetics, now readily accessed because of slower rates. Particle-counting and low-angle light scattering data, both weighted to initial behaviour, are also consistent with this curve. This is depicted in fig. 9 together with a different curve representing the kinetics at long times, as the limiting, apparently constant slopes observed by particle counting.

It is thus evident that the measurement of slow coagulation can be similarly technique-dependent. Since the Fuchs treatment of slow coagulation is strictly a two-particle model, one would expect it to apply only to unambiguous measurements of initial kinetics. Indeed, for the data in fig. 8, the treatment of Duckworth and Lips[14] of the slope and intercept at the critical coagulation concentration yields the estimate of the Hamaker function of 3.3×10^{-21} J, in very good agreement with current theoretical predictions. A similar interpretation of the long-time kinetic data in fig. 9, on the other hand, gives the unrealistic value of 2.2×10^{-20} J.

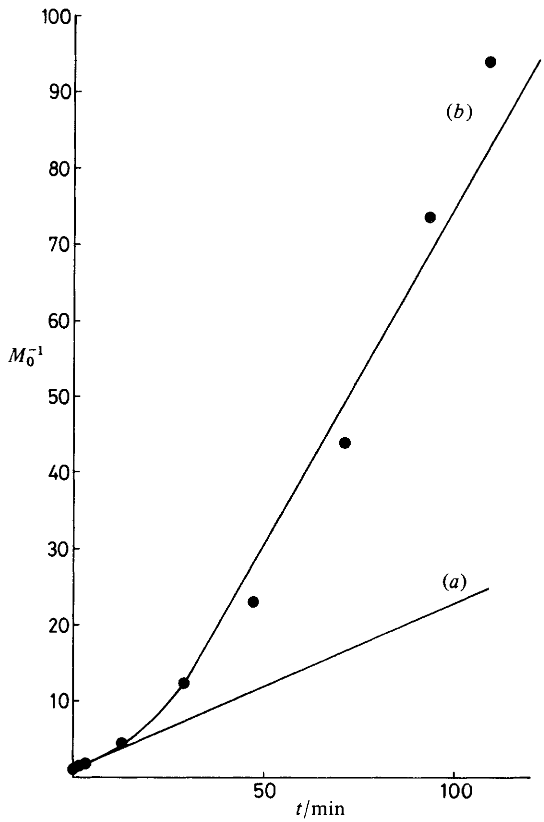

Fig. 5. Intermediate regime of slow coagulation. Variation of inverse zeroth moment $M_0^{-1}(=c_0/\sum_m c_m)$ with time. Full curves represent eqn (3) fitted on basis of common initial slope with functionality f as marked. (25 °C, $c_0 = 3.7\times10^9$ cm^{-3}, 0.075 mol dm^{-3} sodium chloride, latex 167 nm). (*a*) $f = 2.0$, (*b*) $f = 2.15$.

Relevance of Kinetic Theories of Polymerisation

The solutions given by Ziff and Stell[31] for the moments of the RA_f process, in the unidirectional kinetic regime [*i.e.* eqn (1)], are

$$\left.\begin{aligned} M_0 &= 1-f/2[(f\tau/(1+f\tau)] \\ M_1 &= 1 \\ M_2 &= (1+2f\tau)/[1-f(f-2)\tau] \end{aligned}\right\} \quad (3)$$

for reduced times τ less than the gel time $\tau_c = 1/f(f-2)$. Above the gel point, different expressions apply; in the Stockmayer model, in which sol–gel interactions are absent, the solutions are

$$\left.\begin{aligned} M_0 &= 1/[2f(f\tau-\tau_c)] \\ M_1 &= (f-1)\,\tau_c/(f\tau-\tau_c) \\ M_2 &= \infty. \end{aligned}\right\} \quad (4)$$

Theoretical curves based on these equations are shown in fig. 2 for rapid coagulation, where the slope of the initial linear region, most clearly defined for the lowest particle density, was used to define the forward rate constant A^+ and hence τ in terms of t ($\tau =$

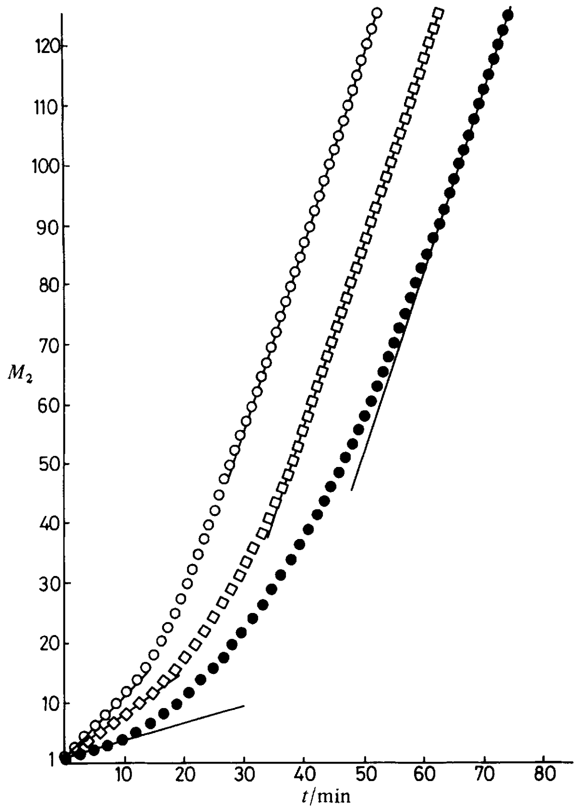

Fig. 6. Typical curvature of low-angle intensity–time traces representing the second moment M_2 ($= \sum_m m^2 c_m / c_0$) of the aggregate distribution in the regime of intermediate slow coagulation. The points are smoothed recorder traces normalised to initial intensity (25 °C, latex 167 nm, $c_0 = 3.7 \times 10^9$ cm^{-3} scattering angle 3°) ○, 0.125 mol dm^{-3}; □, 0.0975 mol dm^{-3}; and ●, 0.0875 mol dm^{-3} sodium chloride. The common final slope represents aggregation in the diffusion limit.

$A^+ c_0 t$). The lack of curvature at the lowest concentration ($c_0 = 2.17 \times 10^7$ cm^{-3}) in fig. 2 is consistent with f either equal to or very close to 2. At higher c_0, each individual set of data does not conform to a single-valued f-functional reaction. However, the analysis clearly suggests a progressive increase in 'effective' functionality with increasing number concentration, and large f (> 3) at the highest densities.

A similar analysis of the slow-coagulation data (intermediate regime of electrolyte adjacent to the critical concentration) in fig. 4 and 5 yields an f value of *ca.* 2.15. Despite the higher number density, accessible because of slower kinetics, the deviations from $f = 2$ are less pronounced than for rapid coagulation, but still indicative of accelerating reactivity; this appears to be a general feature of irreversible colloidal aggregation. It should be noted that the kinetic polycondensation theory is strictly applicable only to reaction-controlled schemes. The processes considered above are reaction-controlled only initially and evolve to become diffusion-limited. This can be inferred from the final slopes in fig. 2, 4 and 5, which all approach the theoretical Smoluchowski value. Lack of divergence in the second moment M_2, represented by low-angle light scattering data in fig. 6, also supports the idea of transition from reaction to diffusion control. In rapid coagulation the initial reaction control could be due solely to hydrodynamic forces,[6,7] and in the intermediate regime of slow coagulation to electrostatic barriers.

The very slow coagulation regime at $C < 0.05$ mol dm^{-3} has quite different kinetic

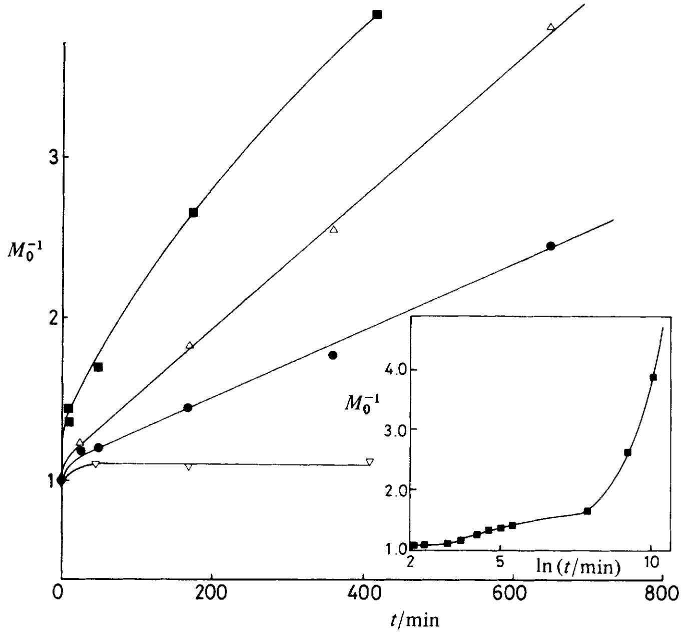

Fig. 7. Dependence of inverse zeroth moment $M_0^{-1}(=c_0/\sum_m c_m)$ on time in the regime of very slow coagulation. ($c_0 = 3.7 \times 10^9$ cm^{-3}, 25 °C, latex 167 nm). Concentrations of sodium chloride (mol dm^{-3}): $\triangledown$, 0.02; ●, 0.03; $\triangle$, 0.035; ■, 0.04. Variation in M_0^{-1} with logarithmic time, including short-time data not shown in fig. 7, is depicted in the insert and suggests two distinct kinetic processes. (For fuller representation of initial kinetics see fig. 10, later).

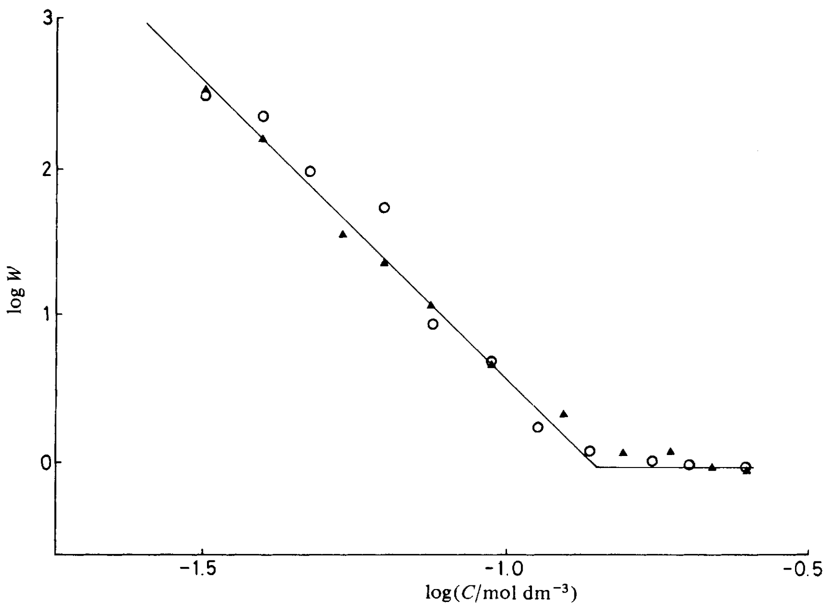

Fig. 8. Log W *vs.* log C stability plot. Initial kinetics measured by time-resolved light scattering at an angle of 30°. (25 °C, latex 167 nm; ▲, $c_0 = 1.25 \times 10^9$ cm^{-3}; ○, $c_0 = 3.75 \times 10^9$ cm^{-3}.)

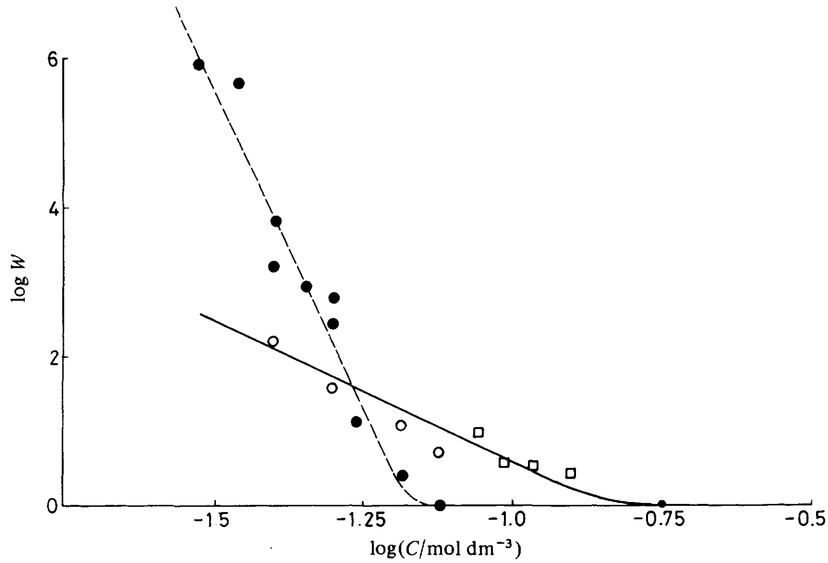

Fig. 9. Importance of timescales in the determination of log W *vs.* log C stability plots. (25 °C, latex 167 nm.) Estimates of W inferred from initial slopes of particle counting measurements (○) and by low-angle light scattering (□), both for $c_0 = 3.7 \times 10^9$ cm^{-3}, are consistent with the full line, which represents the high-angle light scattering data of fig. 8. The final limiting slopes from particle counting experiments (●) result in the steeper stability plot (---).

characteristics from those observed both for rapid coagulation and for the intermediate slow coagulation. A typical representation of the change in M_0 with log t (inset fig. 7) suggests two reasonably separate processes. The initial process is not now one of reaction control accelerating towards a diffusion limit and appears rather as equilibrium control limiting an initial kinetic regime. Assuming this to be the case, we will attempt a quantitative interpretation of the intial step using a treatment of reversible polycondensation by van Dongen and Ernst.[38] The details of this are set out in the Appendix; the theory provides an analytic expression for the time-dependence of the zeroth moment

$$dM_0/d\tau = -1/2(f-2+2M_0)^2 + \beta(1-M_0). \tag{5}$$

If the units of reduced time are chosen in relation to the forward process, as in eqn (2) and (3), $\beta = \exp(b/kT)/c_0$, where b is the standard free energy of bond formation.[32] As shown in the Appendix, b can be related to the osmotic compressibility term

$$G\left\{= c_0 \int_v [g(r)-1]\, 4\pi r^2\, dr\right\}.$$

The radial distribution function $g(r)$ (probability of radial separation r for two particles) defines the spherical potential of mean force $[= -kT \ln g(r)]$; it follows that the present kinetic analysis can be related to familiar colloid interaction potentials.

Fig. 10 shows that the initial stage in very slow coagulation can be well represented by eqn (5) with fitting parameters $f = 2$ and $\beta = 2.7$. The inferred compressibility term G is *ca.* 1 which, by way of illustration, would imply an effective square-well potential of $-16\, kT$ if restricted to a width of 1 Å, alternatively $-12\, kT$ and 50 Å. Expected DLVO secondary minima for the small particles used in this study are too weak (< 0.1 kT) to account for the inferred strength of attraction. It seems more reasonable that a primary minimum is active, but that its combination of depth and width is insufficient to prevent a relatively rapid transition from reaction to equilibrium control. This

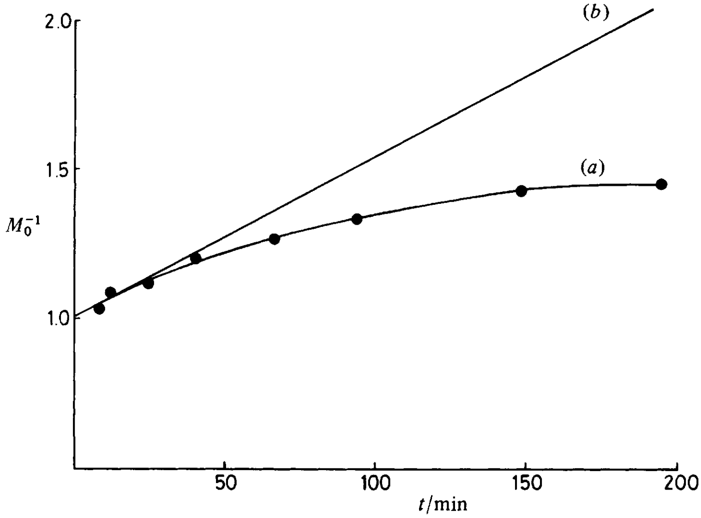

Fig. 10. Typical short-time behaviour of inverse zeroth moment M_0^{-1} in the regime of very slow coagulation. {25 °C, $c_0 = 3.7 \times 10^9$ cm^{-3}; ●, 0.04 mol dm^{-3} sodium chloride. Full lines are fitted on basis of reversible polycondensation theory [eqn (5)] with f and β indicated. The corresponding long-time, irreversible behaviour is shown in fig. 7} (*a*) $f = 2$, $\beta = 2.7$; (*b*) $f = 2$, $\beta \rightarrow 0$.

conclusion applies only to the first reaction step since the the combined process is substantially irreversible because of the second step. The mean number of particles per cluster $p(= M_1/M_0)$ is 1.5 for the first process at 'equilibrium', suggesting the presence of dimers and monomers only; this notion is reinforced by the second process becoming significantly established at $p \approx 2$, at which stage the cumulative mass fraction of aggregates of higher order than dimers has reached 50%. (Despite the involvement of larger aggregates, the second process is not orthokinetic in origin.)

The models of polymerisation kinetics considered here are referred to as random in the sense that the intrinsic 'bond strength' of connected particles is assumed to be invariant with aggregation extent and that ring formation (cyclisation) of particles in clusters does not take place. More complex polycondensation theory [see *e.g.* ref. (39)] would involve such concepts as substitution effect (bond strength dependent on extent of bonding) and cyclisation. While mainly applied to polymers, these ideas are relevant also to the aggregation of spherical colloidal particles, with some interesting differences, however. As pointed out by Cohen and Benedek,[32] spherical colloidal particles, by virtue of spherically symmetric interaction potentials, are expected to be high functional ($f \rightarrow \infty$) reactive units, at least with regard to reaction equilibria. By contrast, the monomers in polymerising macromolecular structures have highly directional, non-spherically symmetric interaction potentials which favour open structures with low probability of 'intra' ring formation. Whereas cyclisation in polymers is important only for large clusters, the effect with spherical colloids can occur as early as the trimer stage (fig. 11). In colloidal aggregation, attractive potentials are generally short-range relative to the size of particles and it is not unreasonable to assume pairwise additivity. Thus, the minimum free energy required to remove a sphere from the cyclised trimeric structure in fig. 11 would be twice that to break a dimer or any of the less compact trimeric structures; in fact, for the ring-closed trimer an effective attractive energy and electrostatic barrier twice that for dimers can be anticipated.

In the light of this argument an attractively simple explanation presents itself for the two-step slow coagulation described above. The first step is indeed effectively limited to dimer formation (more strictly to bonds not involved in formation of threefold rings)

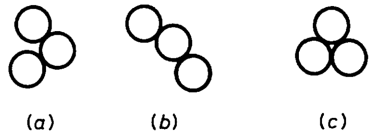

Fig. 11. Ring-closed bonding. Trimer configuration (*c*) is cyclised. Short-range pair potentials imply that the free energy required to break bonds in either (*a*) or (*b*) is equal and half that for (*c*).

and the second process is the formation of higher-order aggregates in close-packed symmetrical configurations with a high incidence, therefore, of closure of threefold rings. The irreversible character of the second process is consistent with the expected doubling in effective attractive energy [$\beta \rightarrow 0$, in eqn (5)]. Moreover, the forward rates (expressed as stability factor log W, which scales approximately linearly with barrier height) are 2.2 for the first stage and 4.4 for the second stage. This supports quantitatively the idea of build up from dimer to ring-closed bonding with doubling in effective pair potentials.

The idea that higher-order aggregates have significantly different growth energetics from those of dimer formation was first suggested by Derjaguin and Kudryavetseva.[18] The view developed here provides quantitative support for this idea. It is also rather a specific description of what could more generally be regarded as a cooperative process with characteristics of 'nucleation' and 'growth'. Implicit in any such description, of course, is the formation of non-random, ordered aggregate structures, and in the following we consider to what extent this is in fact the case.

Aggregate Structure

Direct determination of the radial distribution function $g(r)$, by Fourier inversion of the light scattering structure factor $S(\boldsymbol{Q})$ is not feasible for the ranges of particle size and concentration that can typically be studied by classical kinetic methods.[40] This is because the available range of wavevector $\boldsymbol{Q}$ [$= (4\pi/\lambda)\sin\theta/2$], where λ is the wavelength of light in the dispersion medium and θ is the scattering angle] is then generally insufficient at both high and low Q.

It is possible, however, to match the measured $S(\boldsymbol{Q})$ with model predictions and so gain information on aggregate structure. Lips and coworkers [3,23,24,34] have developed a successful model for the time-resolved structure factor $S(\boldsymbol{Q}, \tau)$ in dispersions coagulating by Smoluchowski kinetics. This can yield information on close-range structure in aggregates[24] and involves the location of maxima in $S(\boldsymbol{Q}, \tau)$ with respect to τ. At such maxima, the average radius $r(\tau)$ of the growing clusters is given by

$$Qr(\tau) = n\pi \quad (n = 1, 2, 3 \textit{ etc.}) \tag{6}$$

where $r(0)$ is the hard-core interaction diameter, d, of the particles. The cumulative coordination number $Z(\tau)$ (average number of neighbours per particle at τ) is

$$Z(\tau) = \sum m(m-1)\, c_m(\tau)/c_0 = M_2 - M_1. \tag{7}$$

Since $M_1 = 1$ in the absence of gelation, and $M_2 = S(0, \tau)$, it follows that $Z(\tau) = S(0, \tau) - 1$. Low-angle measurements, together with the location of maxima in $S(\boldsymbol{Q}, \tau)$ at high Q, can thus characterise the evolution of close-range structure during the initial stages of coagulation. In principle such an approach does not require one to make assumptions about the type of coagulation kinetics. However, it is experimentally very difficult to perform measurements in the low-Q limit; previously therefore the validity of Smoluchowski kinetics was assumed such that $Z(\tau) = 4\tau$.[24]

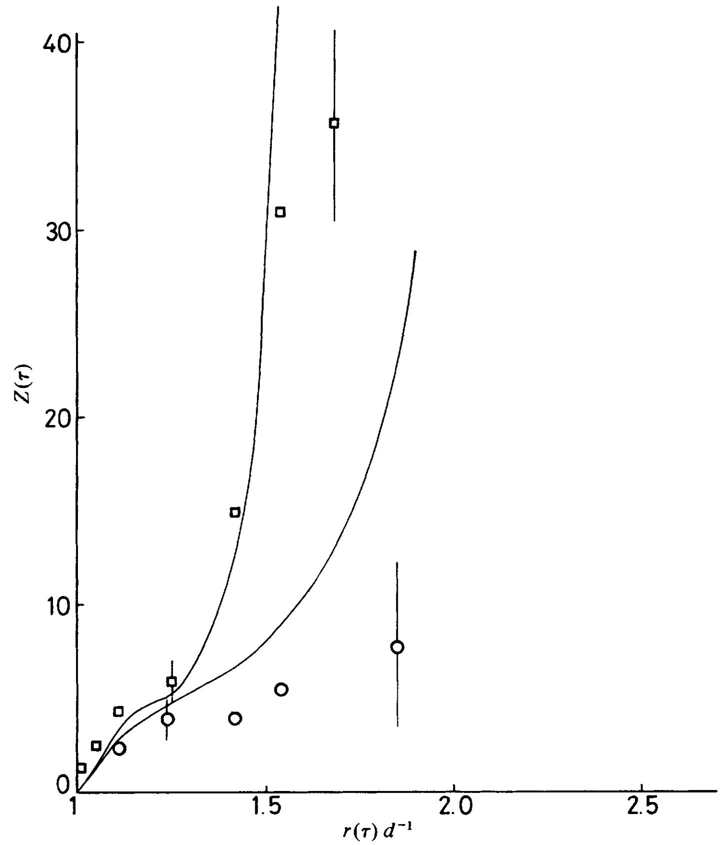

Fig. 12. Dependence of cumulative coordination number $Z(\tau)$ on reduced cluster radius $r(\tau)\,d^{-1}$ in the regime of intermediate slow coagulation. (25 °C, $c_0 = 3.7 \times 10^9$ cm^{-3} latex 167 nm.) Data points obtained by the combination of high- and low-angle scattering measurements: □, 0.0875 mol dm^{-3} and ○, 0.125 mol dm^{-3} sodium chloride. Full curves are the corresponding estimates based on eqn (8) using particle-counting data and the value $f = 2.15$ from fig. 4 and 5.

In view of the evidence presented here of clear deviations from strict Smoluchowski kinetics a more appropriate expression might be

$$Z(\tau) = f^2\tau/[1-f(f-2)\,\tau] \quad \text{[from eqn (3)]}\ [\tau < 1/f(f-2)] \tag{8}$$

with the values of f inferred from the curve fits to the particle-counting data in fig. 2, 4 and 5. This approach is shown in fig. 12 for the intermediate slow coagulation regime. It is apparent that the prediction of $Z(\tau)$ by eqn (3) is in reasonable agreement with the direct measurements by low-angle light scattering (fig. 6). The main conclusion to be drawn, however, is the preference for more compact aggregate structures at lower electrolyte concentrations. This is further seen in fig. 13 in the behaviour of floc size $r(\tau)$ with τ, which is also an indicator of aggregation extent, albeit less directly than $Z(\tau)$. As will be discussed later, it is not unreasonable on both kinetic and statistical-mechanical grounds to expect more compact, less ramified floc structures in solutions of low electrolyte concentration.

Attempts at comparable studies on the effect of particle concentration on floc structure were limited to concentrations $> 2 \times 10^8$ cm^{-3} below which the application of light scattering proved too difficult. In fact to facilitate measurements at low

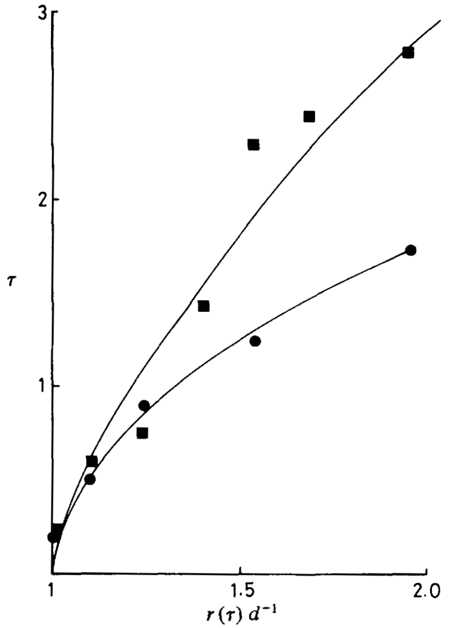

Fig. 13. Reduced time τ *vs.* reduced cluster radius $r(\tau)\,d^{-1}$ in the regime of intermediate slow coagulation. (25 °C, $c_0 = 3.7 \times 10^9$ cm^{-3}; ■, 0.0875 mol dm^{-3} and ●, 0.125 mol dm^{-3} sodium chloride, latex 167 nm.)

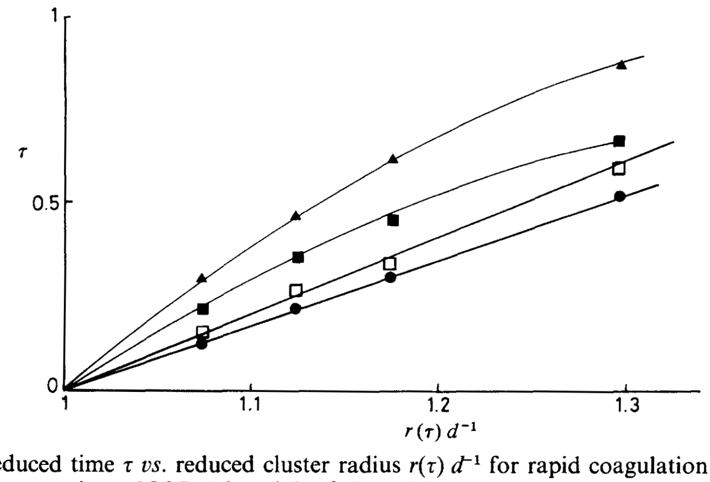

Fig. 14. Reduced time τ *vs.* reduced cluster radius $r(\tau)\,d^{-1}$ for rapid coagulation over a range of particle concentrations. 25 °C, 0.3 mol dm^{-3}, latex 207 nm; particle concentrations c_0 (cm^{-3}): ▲, 3.6×10^8; ■, 7.2×10^8; □, 1.2×10^9; ●, 3.6×10^9.

concentration a latex of larger particle size (207 nm) was chosen. This latex gave a similar dependence of rapid rate constant on particle number concentration as was shown in fig. 2 and 3.

Plots of τ *vs.* $r(\tau)$ in fig. 14 suggest a trend of increasing compactness of flocs with decreasing particle concentration. This is further indicated by the behaviour of the maximum value of $S(\boldsymbol{Q}, \tau)$ with respect to τ at fixed Q ($< \pi/d$). Previous calculations [*e.g.* fig. 6 of ref. (24)] suggest this to be a sensitive indicator of aggregate morphology;

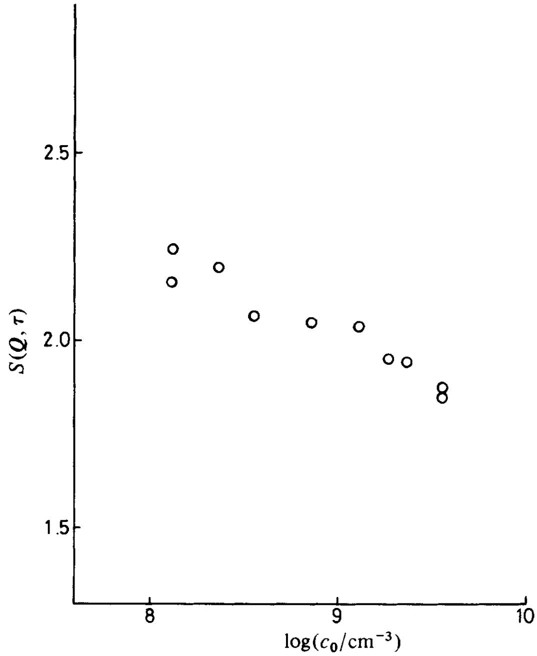

Fig. 15. Dependence of maxima in time-resolved structure factor $S(Q, \tau)$ on particle concentration. Rapid coagulation, 0.3 mol dm^{-3} sodium chloride, latex 207 nm, scattering angle 30°, $Q = 7.9 \times 10^{-3}\ \mathrm{nm}^{-1}$, 25 °C [see also fig. 6 of ref. (24)].

its increase in fig. 15 with decreasing number concentration is consistent with the formation of more compact aggregates at the lower concentrations. The suggested floc structures, in the accessible range of particle concentration, are less compact than those for slow coagulation (fig. 12 and 13); it remains for future investigations to assess whether floc structures, formed at very low particle concentration under rapid conditions, can be comparable in compactness to those formed by kinetics of similar effective functionality (*i.e.* $f \rightarrow 2$) but under obvious reaction control.

Conclusion

The combined kinetic and structural insights suggest the following overall picture. While spherical particles are intrinsically high, functional reactive units with many possibilities of equivalent bonding contacts the statistics and kinetics of such contacts are in general inadequately represented by simple random polycondensation theory in which the bonding is assumed to be independent of extent of aggregation and the formation of cycles is not considered. Interaction potentials of aggregating colloidal particles are short-range and several kT deep. Pairwise additivity and a high incidence of cyclisation can therefore be expected. In fact the latter can occur as early as the trimer stage, since with spherically symmetric potentials there are no steric barriers preventing the closest possible triangular contact between three spheres. Unlike the case for polymers, cyclisation is a preferred process.

The consequence of cyclisation is the deactivation of 'inter'-cluster reactivity in favour of 'intra' bonding. It is sometimes referred to as a process of wastage of functionalities in the sense that intrinsically high functional reactive units display a low effective functionality (approaching 2) in regard to conformity with random polycondensation models. For slow coagulation, the inferred values of 'effective' f are indeed only slightly greater than 2 and the aggregates adopt compact short-range structures consistent with trimeric cycles. Moreover, in the regime of very slow coagulation, the kinetics indicate an initial reversible dimer stage which provides the nucleus for irreversible, trimeric ring-closed bonding.

These inferences would also be consistent with statistical-mechanical reasoning, in so far as short-range order in concentrated systems of spheres is predicted to increase with steepness in hard-core interaction potentials.[41] Unscreened electrostatic potentials in solutions of low electrolyte concentration are more likely to yield ordered structures than those formed by rapid coagulation in excess of electrolyte, and indeed this is observed here.

Statistical aggregation models apply strictly to reaction- or equilibrium-controlled processes and not obviously to diffusion-limited aggregation. For the regime of very slow coagulation, where substantial reaction control is observed, it is not unreasonable to expect a statistical treatment to be relevant, provided the statistical aspects of cyclisation at the trimer stage are adequately incorporated. We hope to report on such a development in the future. It is less clear how to represent kinetic schemes in which the rate is only slightly slower than or equal to the most rapid rate achievable. To illustrate, even under conditions of so-called rapid coagulation the inferred initial rate constant for dimer formation is *ca.* one third to one half of the value expected for diffusion-limited aggregation. Some weak reaction control, possibly attributable to short-range hydrodynamics[6,7] is therefore operative, at least initially. As the aggregation proceeds, the rate accelerates to the diffusion limit. The same qualitative feature is observed with slow coagulation in the regime of electrolyte adjacent to the rapid limit. Since in this case the initial reaction control is clearly electrostatic in origin (and not just hydrodynamic, as might be anticipated for the case of rapid coagulation), it seems a general possibility that diffusion control can follow initial regimes of weak reaction control.

It is clear from the evidence presented that aggregates can rearrange within the timescale of collisions between kinetic units. The rotational correlation time T_R for unhindered rotation of a sphere of radius a is $4\pi a^3\eta/kT$ (s rad^{-1}). The shortest time, T_c, between collisions might be taken as the inverse of the diffusional flux of spheres to a reference sphere ($= 3\pi/8kTc_0$). The ratio $T_R/T_c = (32\pi a^3 c_0/3)$ is typically 10^{-5} in the rapid rate experiments. This would indicate that rearrangement is facile within the timescale of collisions. However, the rearrangement of particles in aggregates involves motion in strongly attractive force fields and it is difficult to estimate the timescale for such hindered rotation. Qualitatively it is reasonable to expect that aggregates are more likely to rearrange in slow coagulation, where collision times are longer and attractive potentials weaker. Rearrangement is less probable in rapid coagulation and at high number concentration. In fact the observed dependence of rapid rate on number concentration would be consistent with the two times being comparable: at $c_0 < 5 \times 10^8$ cm^{-3} the aggregates still have time to rearrange into compact structures and therefore display low effective functionality $f \rightarrow 2$; with increasing c_0 faster collision times progressively prevent rearrangement, leading to open structures with few cycles and higher effective functionality.

In conclusion, deviations from Smoluchowski constant-kernel kinetics have been clearly observed. Their neglect can invalidate the classical interpretation of log W *vs.* log C stability plots. The framework of polycondensation theory has proved to be useful for discussing these deviations. In combination with studies of short-range structure, the importance of rearrangment and cyclisation of spheres in growing aggregates has been elucidated.

Appendix

Kinetics of Reversible Polymerisation

We use the treatment of van Dongen and Ernst,[38] who modify the Smoluchowski equation [eqn (1)] by inclusion of a fragmentation kernel to allow for aggregate break-up,

$$\mathrm{d}c_m/\mathrm{d}\tau = 1/2 \sum_{i+j=m} (K_{ij}\, c_i\, c_j - F_{ij}\, c_m) - \sum_{j=1}^{\infty} (K_{mj}\, c_m\, c_j - F_{mj}\, c_{m+j}) \tag{A 1}$$

where F_{ij} is the rate coefficient for the unimolecular fragmentation process of an m-mer into an i-mer and a j-mer. On the premise that all bonds within an m-mer are equivalent, the total fragmentation rate of the m-mer is proportional to the number of bonds, *i.e.*

$$1/2 \sum_{i+j=m} F_{ij} = (m-1)\exp(b/\boldsymbol{k}T)$$

where b is the free energy of a single bond. This condition, together with a balance condition at equilibrium, leads to the relation between K_{ij} and F_{ij} [see also ref. (32)],

$$F_{ij} = \exp(b/\boldsymbol{k}T)\, K_{ij}\, N_i\, N_j/N_{i+j}. \tag{A 2}$$

The N_j *etc*. are degeneracy factors[32] dependent on the bonding functionality f,

$$N_j = f^j(fj-j)!/(fj-2j+2)!\,j!. \tag{A 3}$$

From eqn (A 2) it follows that

$$-\mathrm{d}\sum c_m/\mathrm{d}\tau = 1/2 \sum_{ij} (K_{ij}\, c_i\, c_j - F_{ij}\, c_{i+j}). \tag{A 4}$$

Changing from concentration scale $c_m(0) = \delta_{m1}$ to $c_m(0) = c_0$, setting $\tau = A^+ c_0\, t$ and $K_{ij} = A^+[(f-2)i+2][(f-2)j+2]$ [see ref. (31)], and substituting eqn (A 2) in eqn (A 4) then yields

$$\mathrm{d}M_0/\mathrm{d}\tau = -1/2(f-2+2M_0)^2 + \beta(1-M_0) \tag{A 5}$$

where $\beta = \exp(b/\boldsymbol{k}T)/c_0$. Note that β depends on initial number density. The solution to eqn (A 5) is

$$M_0 = 1 - \{a - [a + \surd q \tanh(\tau\surd q/2)]/[1 + \tanh(\tau\surd q/2)\, a/\surd q]\}/4 \tag{A 6}$$

where $a = \beta + 2f$ and $q = \beta(\beta+4f)$.

Relationship between 'Bond Free Energy' and Osmotic Compressibility

The bond free energy parameter b [eqn. (5)] can be related to more familiar free energy expressions in colloid science, namely those based on spherically symmetric potentials. Noting that the second moment of the aggregate distribution, M_2, is equivalent to the structure factor $S(Q, \tau)$ in the limit $Q \to 0$, we can write

$$M_2 - 1 = c_0 \int_v 4\pi r^2 [g(r) - 1]\,\mathrm{d}r = G \tag{A 7}$$

where $g(r)$ is the familiar radial distribution function. Since from eqn (3), $M_2 = (1+2f\tau)/[1-f(f-2)\tau]$ and $M_0 = 1 - f/2[f\tau/(1+f\tau)]$, it follows that

$$G = 2f(1-M_0)/[f + 2(1-M_0) - 2f(1-M_0)]. \tag{A 8}$$

$(1-M_0)$ has the significance of 'mean number of bonds' and, through FS theory,[29] is directly related to the fractional extent of reaction, α,

$$\alpha = 2(1-M_0)/f. \tag{A 9}$$

On the basis of equal chemical reactivity, *i.e.* bond strength independent of reaction extent, FS theory requires for an RA_f process that

$$b = -\boldsymbol{k}T\ln\{\alpha/[c_0 f(1-\alpha)^2]\}. \tag{A 10}$$

Combining eqn (A 8) and (A 9) with eqn (A 10) we readily obtain a relation between G and β,

$$\beta = (f/G)(f-2G+fG)/(f-G+fG)$$

or

$$G = Rf/(1+R-Rf); \quad R = 0.5\{2+\beta/f-[(2+\beta/f)^2-4]^{\frac{1}{2}}\} \tag{A 11}$$

where the dimensionless parameter $\beta = \exp(b/\boldsymbol{k}T)/c_0$ can be inferred from kinetic data by fitting to eqn (A 6).

Finally, a comment on standard states: Our choice of concentration units for c_0 (particles per unit volume) implies that $b/\boldsymbol{k}T$ is not dimensionless. Cohen and Benedek[32] define a dimensionless bond free energy $g/\boldsymbol{k}T$ using mole fraction units, X_0, in connection with eqn (A 10). To an excellent approximation, $X_0 = c_0 v_s/N$, where v_s is the molar volume of solvent and N is Avagadro's number; it is readily shown that $b = g+\boldsymbol{k}T\ln(N/v_s)$. Also $\exp(b/\boldsymbol{k}T)/c_0 = \exp(g/\boldsymbol{k}T)/X_0 = \beta$. The distinction is therefore not important if the sole objective is to determine G, as this depends only on the dimensionless parameter β, which is common to both standard states.

References

1 M. von Smoluchowski, *Z. Phys. Chem.*, 1917, **92**, 129.
2 J. W. Th. Lichtenbelt, C. Pathmamanoharan and P. H. Wiersema, *J. Colloid Interface Sci.*, 1974, **49**, 281.
3 A. Lips and E. Willis, *J. Chem. Soc., Faraday Trans. 1*, 1973, **69**, 1226.
4 W. Hatton, P. McFadyen and A. L. Smith, *J. Chem. Soc., Faraday Trans. 1*, 1974, **70**, 655.
5 P. McFadyen and A. L. Smith, *J. Colloid Interface Sci.*, 1973, **45**, 573.
6 L. A. Spielman, *J. Colloid Interface Sci.*, 1970, **33**, 562.
7 E. P. Honig, G. J. Roeberson and P. H. Wiersema, *J. Colloid Interface Sci.*, 1971, **36**, 97.
8 N. Fuchs, *Z. Phys.*, 1934, **89**, 736.
9 H. Reerink and J. Th. G. Overbeek, *Discuss. Faraday Soc.*, 1954, **18**, 74.
10 R. H. Ottewill and J. N. Shaw, *Discuss. Faraday Soc.*, 1966, **42**, 154.
11 A. Watillon, M. Romerowski and F. van Grunderbeeck, *Bull. Soc. Chim. Belg.*, 1959, **68**, 450.
12 A. Watillon and A-M. Joseph-Petit, *Discuss. Faraday Soc.*, 1966, **42**, 143.
13 A. Bleier and E. Matijevic, *J. Colloid Interface Sci.*, 1976, **42**, 143.
14 R. M. Duckworth and A. Lips, *J. Colloid Interface Sci.*, 1978, **64**, 311.
15 R. Zsigmondy, *Z. Phys. Chem.*, 1917, **92**, 600.
16 A. Westgren and J. Reitstotter, *Z. Phys. Chem.*, 1917, **92**, 750.
17 P. Tuorila, *Kolloidchem. Beih.*, 1926, **22**, 191.
18 B. V. Derjaguin and N. M. Kudryavetseva, *Colloid J.*, 1964, **26**, 49.
19 G. K. von Schulthess, G. B. Benedek and R. W. de Blois, *Macromolecules*, 1980, **13**, 939.
20 H. Gedan, H. Lichtenfeld and H. Sonntag, *Colloid Polym. Sci.*, 1982, **260**, 1151.
21 P. G. Cummins, E. J. Staples and L. G. Thompson, *J. Colloid Interface Sci.*, 1983, **92**, 189.
22 M. S. Bowen, M. L. Broide and R. J. Cohen, in *Kinetics of Aggregation and Gelation*, ed. F. Family and D. P. Landau (Elsevier, Amsterdam, 1984), p. 185.
23 A. Lips, C. Smart and E. Willis, *Trans. Faraday Soc.*, 1971, **67**, 2979.
24 D. Giles and A. Lips, *J. Chem. Soc., Faraday Trans. 1*, 1974, **74**, 733.
25 P. G. Cummins, E. J. Staples and L. G. Thompson, *J. Colloid Interface Sci.*, 1983, **92**, 287.
26 E. M. Hendriks and M. H. Ernst, *J. Colloid Interface Sci.*, 1984, **97**, 176.
27 M. H. Ernst, R. M. Ziff and E. M. Hendriks, *J. Colloid Interface Sci.*, 1984, **97**, 266.
28 H. Dostal and R. Raff, *Z. Phys. Chem., Teil B*, 1936, **32**, 47.
29 W. H. Stockmayer, *J. Chem. Phys.*, 1943, **11**, 45.
30 K. Dusek, *Polym. Bull.*, 1979, **1**, 523.
31 R. M. Ziff and G. Stell, *J. Chem. Phys.*, 1980, **73**, 3492.
32 R. J. Cohen and G. Benedek, *J. Phys. Chem.*, 1982, **86**, 3696.
33 M. S. Bowen, M. L. Broide and R. J. Cohen, *J. Colloid Interface Sci.*, 1985, **105**, 617.
34 A. Lips, *J. Chem. Soc., Faraday Trans. 2*, 1987, **83**, 221.

35 K. Kajiwara, W. Burchard and M. Gordon, *Br. Polym. J.*, 1970, **2**, 110.
36 K. Kajiwara and M. Gordon, *J. Chem. Phys.*, 1973, **59**, 3623.
37 A. Kotera, K. Furusawa and Y. Takeda, *Kolloid Z.*, 1970, **239**, 677.
38 P. van Dongen and M. H. Ernst, *J. Phys. A*, 1983, **16**, L327.
39 K. Dusek, *Br. Polym. J.*, 1984, **17**, 185.
40 W. A. House, *J. Chem. Soc., Faraday Trans. 1*, 1978, **74**, 1112.
41 J. D. Bernal, *Proc. R. Soc. London, Ser. A.*, 1964, **280**, 299.

Paper 7/1067; *Received* 16*th June*, 1987